View metadata, citation and similar papers at core.ac.uk
brought to you by CORE
provided by NASA Technical Reports Server

N79-16778

VOYAGER RADIO OCCULTATION INVESTIGATIONS AT SATURN

G. L. Tyler and V. R. Eshleman

Radioscience Laboratory, Stanford University
Stanford, California 94305

ABSTRACT

Voyager will use dual-frequency 3.5 and 13 cm wavelength radio occultation techniques to study the atmospheres and ionospheres of Saturn and Titan, and the rings of Saturn. At Titan radio occultation is predicted to probe the atmosphere to the surface. The existence of a surface could be confirmed by detection of an obliquely scattered echo. At Saturn the two Voyager encounters will provide occultation measurements of temperate and equatorial regions of the atmosphere and ionosphere, and of the rings. The atmosphere will also be probed in polar regions during the deepest portions of the occultation. Both frequency and intensity data will be collected and jointly analyzed to study temperature-pressure profiles, and to derive information on atmospheric shape, turbulence, and "weather". For the rings, Voyager will provide measurements of the complex (amplitude and phase) radio extinction and angular scattering functions of the ring particles as a function of wavelength, polarization, and radial distance from Saturn. These observations will be used to infer the first several moments of the ring particle size distribution, the total amount of material in the rings, the radial distribution of material, and limits to possible particle shapes and constituents.

The Voyager radio occultation investigations discussed here are based on the use of the 3.5 and the 13 cm wavelength spacecraft transmitters and ground receiving systems which are also used for telecommunications. These studies are directed towards the atmospheres and ionospheres of Saturn and Titan, and the rings of Saturn. A number of other investigations are also planned, but will not be discussed here (Eshleman *et al.*, 1977).

Salient features of these investigations are the use of: a) harmonically related frequencies at the two wavelengths, b) considerably higher power levels than previous experiments, c) a new, radiation-hardened, highly stable spacecraft frequency standard, and d) improved phase, group-delay, and amplitude stabilities in spacecraft and ground radio systems. The resulting experimental precisions are given in Table 1.

When a spacecraft moves behind a planet as viewed from Earth, the radio path traverses the planet's atmosphere and ionosphere, and for Saturn, will also probe its system of rings. All of these regions affect the characteristics of the received radio signals, making possible the study of the vertical structure of these atmospheric regions, clouds, small and large scale variations associated with turbulence and weather, and fundamental characteristics of the ring particles and their disposition around Saturn. The atmosphere and ionosphere of Titan will also be studied by such occultation measurements. It is also expected that a reflection from the surface of Titan near the limb will be obtained during the occultation measurements. If this occurs, it will provide positive confirmation that the measurements reach the surface.

Table 1. Voyager Occultation Experiments at Saturn

Wavelength (cm)	S/N (1 s)	$\Delta P/P$(1000 s)	$\Delta f/f$(1 s)
3.5	6.3×10^4	<10%	2×10^{-12}
13	2.5×10^3	< 1%	2×10^{-12}

ATMOSPHERES

Saturn

Flyby trajectory characteristics of the two Voyager spacecraft at Saturn provide a good combination of conditions for radio occultation studies of its atmospheres and ionospheres. Figure 1 illustrates the paths of the radio image of the spacecraft as seen from Earth for the nominal JST and JSX trajectories. Note that both equatorial and polar regions will be probed, and that there will be both a near-central occultation and a more grazing occultation in which the spacecraft sets or rises, as seen from the Earth at large angles from the local vertical at the occulting body. Figure 2 provides a side

ORIGINAL PAGE IS
OF POOR QUALITY

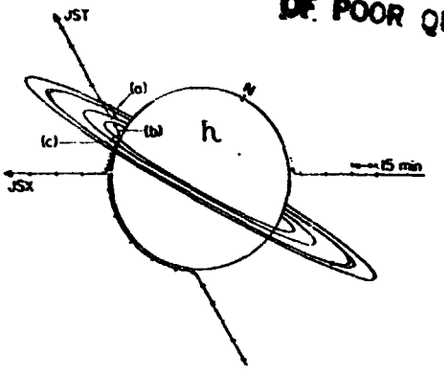

Figure 1. View from Earth of Voyager occultations at Saturn — *The spacecraft radio images follow the indicated paths for the JST and JSX trajectories at Saturn. Note that there is a near central and more grazing occultations. For JST at Saturn, region (a) provides a clear occultation of the rings and (b) a clear atmospheric occultation, while (c) is a combined ring and atmospheric occultation.*

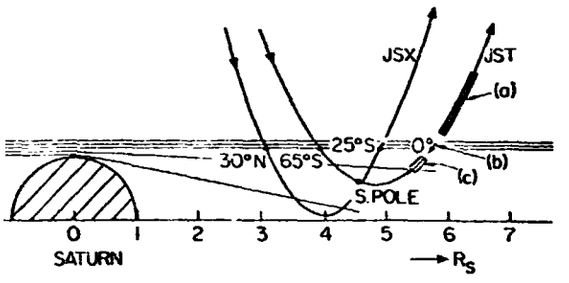

Figure 2. Side view of Voyager occultations at Saturn — *The trajectories are plotted in a rotating plane that instantaneously contains the earth, the spacecraft, and the center of the planet. The latitudes of occultation immersions and emersions are shown, and regions (a), (b), and (c) of Figure 1 are also illustrated here.*

view of the occultation geometry in a rotating plane that instantaneously contains the Earth, the spacecraft, and the center of Saturn. The figure is illustrated to scale. Occultation distances from the planetary limb to the spacecraft range about 3 to 6 R_S (Saturn radii).

For a central passage of a spacecraft behind Saturn, the trajectory would dip to zero in the vertical scale of Figure 2. At occultation entry and exit, the spacecraft would appear from the Earth to set and rise approximately normal to the limb of the planet, and the atmosphere would be sampled with height along a near-vertical path. Such a central passage is the optimum condition for occultation measurements of the vertical structure of the atmosphere. The JSX (Uranus) trajectory at Saturn is near optimum in this regard, while the JST trajectory gives occultation conditions in which the virtual image of the spacecraft enters the atmosphere along a path well away from the vertical. After modest penetration into the atmosphere, the image of the JST spacecraft, as viewed from Earth, will move approximately horizontally through the atmosphere, over south polar regions of Saturn, with spacecraft rise at emersion being over the equator in the western ansa. While such a non-central occultation will provide reliable vertical profiles over a smaller range of heights than is the case for central occultations, it is expected to be very useful in sampling conditions over a wide range of latitudes, in studying complex atmospheric structure due to turbulence and weather, and in helping to determine possible distortion of gravitational equipotentials from oblate spheroids, as discussed below.

Figure 2 shows illustrative radio ray paths in the regions behind Saturn. Measurements of the received frequency of the radio signals from the spacecraft provide precise information on the angle of refraction in the atmosphere. Knowledge of this angle as function of time, together with the spacecraft trajectory, makes it possible to estimate the refractivity of the atmosphere as a function of height. (Refractivity $\nu = n-1$, where n is the refractive index.) The profile of refractivity in turn can be used to determine the relative temperature and pressure as a function of height, and such relative profiles can be made absolute from knowledge of the atmospheric constituents (Fjeldbo and Eshleman, 1965; Kliore *et al.*, 1965; Eshleman, 1965).

The process of converting the observed signal frequencies into a height profile of refractivity, or a more general two or three dimensional refractivity model of the atmosphere, is not straightforward and in general cannot yield a unique result. The problem of determining refraction angles from any given atmospheric model is, by comparison, both straightforward and unique.

If one imposes the assumption that the atmosphere is spherically symmetric, there is a mathematical transform pair that allows computations in either direction, and in this case the profile computed from the refraction angles is the correct and only answer (Fjeldbo *et al.*, 1971). We are not aware of any other potentially applicable model where such a direct mathematical inversion has been identified. A different approach involves iteration downward in an atmosphere modeled by successive thin layers within each of which the refractivity is constant. While such a method has been used for the spherical case (Fjeldbo and Eshleman, 1968), it is potentially applicable with further development to any geometrical complexity that can be modeled in this way. The radio science team is preparing for both types of inversion approaches for the Voyager occultation experiments. The departure from spherical symmetry due to the oblateness of the major planets will be treated both by using a sequence of offset spherically-symmetric models to match the curvature of the equi-refractivity profiles at the occultation points (Kliore and Woiceshyn, 1976), and by the iterative process applied to the oblate spheroidal geometry. It is expected that this latter method may be made more complete with attempts to treat possible zone-belt differences and particular spot features in the atmospheres.

Important additional information about atmospheric structure can be obtained from the intensity of the dual-frequency signals received during occultation. Figure 2 illustrates the effects of differential refraction on intensity by showing that evenly spaced parallel rays to Earth connect with increasingly spread rays at the spacecraft for progressively lower ray passages through the atmosphere. Thus signal intensity decreases as the rays penetrate deeper into the atmosphere. Measured signal intensity can be inverted as discussed above for the frequency measurements, and should yield the same refractivity profiles if the changes in intensity are due solely to such atmospheric defocussing (Fjeldbo *et al.*, 1971). However, there are two other factors to consider, as discussed below.

Certain errors in profiles derived from Doppler frequency measurements undergo an inherent magnification deep in the atmosphere, but this does not occur in the intensity inversion process (Hubbard *et al.*, 1975; Eshleman, 1975). Thus cross-checks can be made to determine the onset of such magnified errors, with the possible result that the characteristics of such an error source could be measured. For example, profiles determined from Doppler measurements during the non-central occultations will be very sensitive to the assumed orientation of the local vertical (Hubbard *et al.*, 1975). At atmospheric levels where the signal intensity is reduced by a factor M (which could

reach values of thousands), an error in the local vertical of δ radians would produce a temperature error on the order of 200 Mδ% when the spacecraft sets or rises at an angle of 45° from the vertical (Eshleman, 1975). But if the temperature were known more accurately than this from the intensity measurements, or from other Voyager experiments, then the apparent error could provide information on the orientation of local equipotentials to an accuracy which could be important in the study of gravitational anomalies due to internal structure and atmospheric currents. The accuracy of the local vertical of the global gravity field of Jupiter as determined with Pioneer spacecraft is about one minute of arc (Anderson, 1976).

The second factor relative to the use of signal intensity measurements is that atmospheric absorption would add logarithmically to defocussing loss, but these two effects would be separable whenever the refractivity profile can be determined from the Doppler measurements (Fjeldbo *et al.* 1971). Microwave absorption in the atmosphere is expected due to cloud condensates, their vapors, or principal atmospheric constituents at low altitudes and hence high densities. The loss profile measured at the two radio frequencies would provide information on the location, density, and other characteristics of the clouds or other absorbing material.

Before absolute pressure and temperature profiles can be derived from the refractivity data, one must know either the composition or the temperature at some altitude level. For the Voyager missions, the IR and UV sensors are expected to yield complementary data on these parameters. Additional information may be obtained from the signal intensity measurements. For instance, if the altitude level of ammonia clouds could be identified in a microwave loss profile, one would know the approximate temperature at this altitude based on considerations involving vapor saturation. This temperature information would, in turn, allow us to use the scale height of the refractivity profile near the cloud level to estimate the mean molecular mass of the atmosphere. The mean molecular mass could in turn be utilized together with other data to establish limits on the abundance ratios between the principal atmospheric constituents.

Titan

The atmospheric occultation experiment is of special interest for Titan, the only satellite known to have an appreciable atmosphere. The trajectory for the JST mission includes a near-central passage behind Titan, under conditions which are

favorable for vertical profile measurements. The same general considerations discussed above also apply at Titan, except that oblateness is not expected to be important. While there is considerable uncertainty about atmospheric conditions at Titan (Hunten, 1974), it is expected that the radio occultation experiment can provide important atmospheric results over a wide range of altitudes, probably including conditions from the surface to heights where the atmospheric pressure is on the order of 1 mbar. At greater heights, ionospheric measurements would provide additional information as discussed below.

We have computed the radio propagation effects of the four model atmospheres of Titan (Paul Weisman, JPL; private communication) with the results that are summarized in Table 2 and Figure 3. In Table 2, the important parameters to compare are those for surface pressure, pressure for critical refraction, the near-limb signal

Table 2. Summary of Model Titan Atmospheres and Their Radio Effects

Model / Name	I Danielson	II Hunten	III Divine	IV Sagan
Principal Constituent	CH_4	N_2	N_2	Ne
Amount (km-A)	1.6	25	60	20
Second Constituent)	-	CH_4	CH_4	CH_4
Amount (km-A)	-	0.08	0.19	0.08
Scale Height (km)	31	18	28	66
Temperature (K)	76.0	76	122	204
Surface Pressure (bar)	0.015	0.40	0.96	0.23
Pressure for critical refraction (bar)	7.3	6.2	15.9	275
Near-limb signal (dB)	-13	-16	-14	-10
Bending angle at surface (radian)	5.36^{-4}	1.31^{-2}	1.54^{-2}	3.26×10^{-4}
Critical distance for a near limb maneuver (meters)	5.04^{9}	2.06^{8}	1.75^{8}	$8.27 \times 10^{+9}$

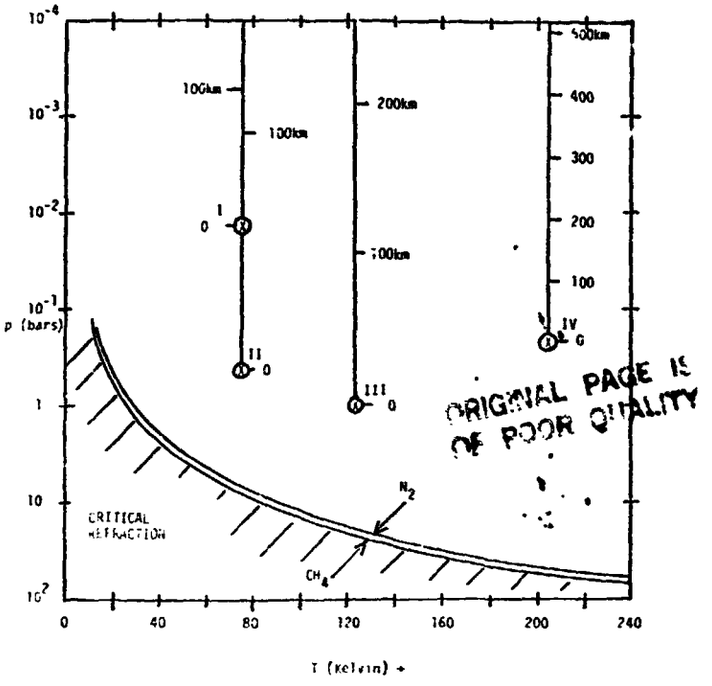

ORIGINAL PAGE IS
OF POOR QUALITY

Figure 3. p-T Occultation space at Titan — *Figure illustrates the relationship of four model atmospheres (I-IV, see Table II) to the expected critical refraction level at Titan. Since critical refraction depends on the specific refractivity of the actual constituents, two illustrative cases, for pure atmospheres of N_2 and CH_4, are given.*

loss, bending angle at the surface and the critical occultation distance. Surface pressure and pressure for critical refraction compare the expected surface pressure with the pressure at the height at which the radius of curvature of a horizontal ray equals the radius of the ray. In all cases the critical height occurs at a level in the atmosphere that is more than one order of magnitude pressure greater depth than the expected surface pressure. The difference in these two pressures is the theoretical margin for occultation measurements to reach the surface.

In practical cases, signal strength must be considered as well. The entry under near-limb signal loss indicates the maximum signal loss due to atmospheric defocussing that will be encountered during occultation while observing signals from the closest limb of Titan. The difference between this loss and the initial signal-to-noise ratios (see Table 1) is available for study of absorption and scattering of the ray. Note that this difference typically is between two and three orders of magnitude in signal strength. To date, no potentially large sources of absorption have been identified.

The remaining two quantities indicate the margins for a successful no-limbing tracking, or a near-limb tracking maneuver occultation. The bending angle at the surface is always less than the Voyager 13 cm -3 dB half-beam width of 2.1×10^{-2} radians, although it can be larger than the -3 dB half-beam width of 5.9×10^{-3} radians at 3.5 cm wavelength. The critical distance is the maximum flyby distance at which a near-limb tracking maneuver can successfully track a surface ray. The Voyager occultation distance is planned to be about 3×10^{7} m, or about one order of magnitude less than the smallest value obtained for this quantity. At present the Voyager Radio Science Team plans to track the closest limb throughout the occultation.

Figure 3 illustrates the relationship of these models to the critical refraction levels of pure N_2 and CH_4. This figure allows easy estimation of proposed atmospheres to the critical occultation level.

Ionospheric Profiles

The vertical profiles of free electron concentration in an ionosphere can be found from the profile of refractivity, which in turn is determined in the same general way as described previously for the refractivity of the neutral atmosphere. However, there is an important difference in that the refractivity is also proportional to the square of the radio wavelength for ionospheres, while it is essentially independent of wavelength for neutral atmospheres. Thus the dual frequency measurements will be self-calibrating in the sense that ionospheric profiles derived from Doppler frequency differences will be independent of trajectory uncertainties and spacecraft oscillator instabilities (Fjeldbo *et al.* 1965). Ionospheric profiles will be obtained in conjunction with the atmospheric occultations at both Saturn and Titan.

RINGS OF SATURN

The Voyager encounters with Saturn provide an opportunity to study the ring system with radio occultation techniques. The JST trajectory includes a Saturn ring occultation following atmospheric occultation emersion. The JSX trajectory provides an optional retargeting for Titan encounter and ring occultation should the JST spacecraft fail prior to Saturn encounter.

The goals of these observations are to measure the complex (amplitude and phase) radio extinction and angular scattering function of the rings as a function of wavelength, polarization, and radial distance from Saturn. These observations would then be used to infer the first several moments of the ring particle size distribution, the total amount of material in the rings, the radial distribution of that material, and limits to possible particle shapes and constituents (Marouf, 1975).

As in atmospheric occultations, the 13 and 3.5 cm-λ radio waves will be transmitted from the spacecraft through the rings and received at Earth. The motion of the spacecraft will carry the geometric line of sight from the planetary occultation point within the western ansa (region (b) in Figures 1 and 2) outward through the entire ring system (region (a) in the figures). The complete phase, intensity, and polarization of the received signals at both wavelengths will be recorded at Earth. Note also from the figures that the complete ring plane will be crossed along a second path by the rays refracted through the atmosphere just prior to the atmospheric emersion of the spacecraft image (region (c) in the figures). This combined atmospheric and ring occultation will also be recorded.

It is expected that the received signal will consist of two principal components; a coherent signal that represents propagation directly through the rings, and an incoherent component which reaches the earth by scattering from particles that do not lie along the geometric straight-line path to Earth (Eshleman, 1973). Even though the rings consist of discrete particles, they interact with the radio wave in such a way as to produce average effects (per unit volume) on wave intensity and phase, much as does an atmosphere or ionosphere of discrete molecules or electrons. For the coherent signal, the rings can be characterized by their effective wave propagation constants. The coherent and incoherent components will be recognized and separated in the data on the basis of their spectral, time correlation, and polarization characteristics.

The first-order effects expected are shown in Figure 4. At each wavelength, the coherent component will be shifted in phase and attenuated due to the effective propagation constants of the ring material. If the concentration of ring particles varies with radial distance from Saturn, the progressive change in phase would correspond to small changes in the angle of refraction, so that it appears as a frequency shift in a manner that is analogous to an atmospheric occultation. Unlike atmospheric occultation, however, the reduction in the coherent signal intensity in ring occultation is expected to be due primarily to scattering of energy out of the direct path.

The phase of the coherent wave depends primarily on the total number of small particles per unit area projected normal to the spacecraft-to-Earth line-of-sight (i.e., the areal density). The precision of the phase data is limited by the oscillators employed. For frequency stabilities associated with the onboard oscillator, the threshold of detection would correspond to small ice particles whose areal density varies by about 20 g/cm^2 in a period of about 1000 s. Assuming a spacecraft velocity of 10 km/s in the plane of the sky, this gives a sensitivity to gradients in material of 2×10^{-3} $g/cm^2/km$, if the particles are small as compared with the radio wavelength.

The intensity of the coherent wave also carries important information about the ring particles. It appears that measurements of coherent signal extinction will be limited to an accuracy of about 10% at 3.5 cm-λ, and perhaps 1% at 13 cm, by systematic and slowly varying errors in spacecraft antenna pointing. For a simple model involving only optically thin regions and particles that are large relative to the wavelength, these errors would correspond to the same fractional error in the total projected area of the particles viewed against the plane of the sky. We estimate from current models for the B ring that this attenuation will be between 40 and 60 dB. As a result, the coherent wave may be below the limit of detection during portions of the ring occultation.

The incoherent signal illustrated in Figure 4 arises from scattering by ring particles with circumference greater than a wavelength. It can be analyzed in terms of the average angular scattering properties of the rings mapped into the frequency domain by the Doppler effect. This mapping can be understood in terms of the relative velocities between the spacecraft, ring particles, and the receiving station on Earth. Signals transmitted from the spacecraft illuminate ring particles at a frequency shifted by the instantaneous relative spacecraft-particle velocities. The component of the

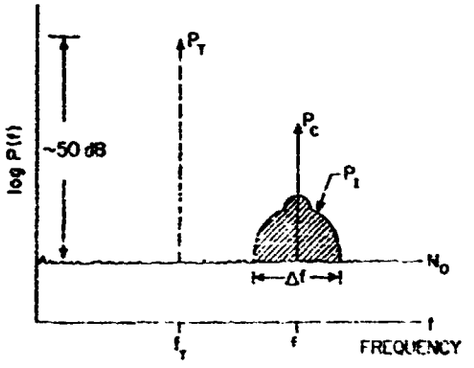

Figure 4. Signal characteristics during Saturn ring occultation — *Transmitted signal (P_T,f_T) is converted into coherent part (P_c,f_c) and incoherent part (P_I, Δf). System noise level N_0 is about 50 db below the received power in the absence of rings. Shape of incoherent spectrum schematically represents expected signature of a bimodal particle size distribution. Most scattering effects are wavelength dependent so that additional information is available by comparison of 13 and 3.5 cm results. Variation of incoherent spectrum with polarization is not illustrated.*

scattered wave that is re-radiated in the direction of the earth undergoes a second shift in frequency determined by the velocity of the particle relative to that of the Earth. The JST trajectory at Saturn was chosen in part so as to align the loci of constant Doppler shifts with the circumferential ring coordinate over a limited region of the ring plane. An example of one such set of Doppler loci is shown in Figure 5. As illustrated, each slice of the incoherent spectrum is closely associated with a portion of the rings at a constant radius from Saturn's center of mass. We estimate that the radial resolution achieved at 3.5 cm wavelength will be about 100 km, approximately 2% of the radial dimension of the Cassini division between the A and B rings. At 13 cm the resolution will be somewhat poorer due to the larger ring area illuminated at the longer wavelength, and the deviation of the Doppler loci from the ideal condition over the larger area.

A critical factor in the ring occultation experiment is the size of the particles relative to the size of the spacecraft antenna (3.66 m diameter). If the predominant particle size is greater than the spacecraft antenna size, then the forward scattering lobe will be narrower than the spacecraft antenna beamwidth. In this case, most of the scattered energy can be observed with a simple geometry in which the spacecraft antenna is always directed toward the geometric position of the Earth. However, particles smaller than the spacecraft antenna will produce forward diffraction lobes that are wider than the antenna beamwidth and no fixed condition of illumination will permit measurements of the entire scattering lobe. Current Earth-based radar observations indicate that many particles larger than about 2 cm in diameter are present in the rings, but give little hard information to constrain the upper size limits (Pollack *et al.* 1973). We cannot now predict which of the alternatives above best represents the conditions we will encounter or even if such conditions will be the same for all parts of the ring system.

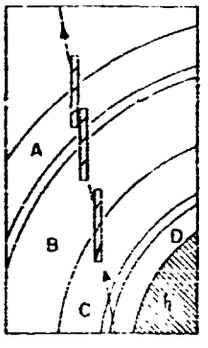

Figure 5. Radial resolution for incoherent signals in Saturn ring occultation measurements — *Figure represents ring plane with Saturn at lower right. Spacecraft is located below the plane of the rings out of the figure at the top of the page, earth above the ring plane out of the figure at the bottom of the page. Directed line from lower right to upper left is the path of the geometric ray between spacecraft and the earth. Boxes outline the ring plane area illuminated at three instants by the 3.5 cm antenna pattern. The one-half power contour is approximately an ellipse with axes given by the rectangle. Curved lines approximately tangent to the circumferential coordinates of the rings are loci of constant Doppler shift separated by 1 kHz. Measurement resolution is on the order of 20 Hz. Similar figure obtains at 13 cm wavelength except antenna beam intersection is larger and contours deviate from circumferential condition.*

The radio science team is planning to conduct the JST ring occultation experiment with the antenna directed toward the Earth. This strategy will yield the maximum signal-to-noise ratio for the coherent component. It will also yield the mean particle size and information on the particle size distribution, particularly if most of the particles are a few meters in diameter or larger. The effects of particles in the centimeter-to-meter size range will be recognizable in the data, although detailed information will not be available on the distribution of sizes in that range. We hope to obtain information on the intermediate-scale particles by incorporating an oblique scatter experiment in the JSX flyby, during which the spacecraft antenna will be directed toward the rings through a range of oblique scattering angles, but the feasibility of this has not yet been completely determined.

Polarization of the scattered waves is an independent observable which is germane to the study of the incoherent signal, and in principle, to the coherent wave as well. The polarization of the coherent wave will be modified by factors that depend primarily on particle shape if multiple scatter can be neglected, and by a combination of particle shape and multiple scattering in regions where the latter is important. Strong depolarization is observed in backscatter radar observations, and is one of the puzzling aspects of the ring system in these Earth-based experiments (Goldstein et al., 1977). For the coherent wave, we know of no particular reason to expect strong polarization effects, but this could occur if non-spherical particles have ordered orientations.

Polarization measurements will be made with coherent receiving systems for right and left hand circular polarization at each wavelength. The data can be processed to determine the complete properties of the waves -- intensity, axial ratio and orientation of the polarized part, and the intensity of the unpolarized part -- as a function of time and frequency. For the coherent signal, data processing based on polarization will improve the a posteriori signal-to-noise ratio.

The discussion above is expressed in terms of a simplified, single-scattering model. However, the fundamental experimental considerations of geometry and strategy do not depend on that model, but only on the assumption that the particles follow individual Keplerian orbits with few collisions. We expect to encounter a wide range of conditions as the radio beam moves outward through the ring system, and there may be no single scattering model or analysis technique which is appropriate over the full range. We are engaged in a continuing study of this experiment with emphasis on the sensitivity of data inversion to the experimental parameters, and on more complex models which include multiple scatter and polarization.

REFERENCES

Anderson, J. (1976). The gravity field of Jupiter. In *Jupiter* (T. Gehrels, ed.), pp. 113–121. University of Arizona Press, Tucson.

Eshleman, V. (1975). Jupiter's atmosphere: Problems and potential of radio occultation. *Science 189*, 876–878.

Eshleman, V. (1973). The radio occultation method for the study of planetary atmospheres. *Planet. Space Sci. 21*, 1521–1531.

Eshleman, V. (1965). Radar astronomy of solar system plasmas. In *Solar System Radio Astronomy*, (J. Aarons, ed.), pp. 267–293. Plenum Press, NY.

Eshleman, V., Tyler, G., Anderson, J., Fjeldbo, G., Levy, G., Wood, G., and Croft, T. (1977). Radio science investigations with Voyager. *Space Sci. Rev. 21*, 207–232.

Fjeldbo, G., and Eshleman V. (1968). The atmosphere of Mars analyzed by integral inversion of the Mariner IV occultation data. *J. Planet. and Space Sci 16*, 1035–1059.

Fjeldbo, G., and Eshleman, V. (1965). The bistatic radar-occultation method for the study of planetary atmospheres. *J. Geophys. Res. 70*, 3217–3226.

Fjeldbo, G., Kliore, A., and Eshleman, V. (1971). The neutral atmosphere of Venus as studied with the Mariner V radio occultation experiments. *Astron. J. 76*, 123–140.

Goldstein, R., Green, R., Perrengill, G., and Campbell, D. (1977). The rings of Saturn: Two frequency radar observations. *Icarus 30*, 104–110.

Hubbard, W., Hunten, D., and Kliore, A. (1975). Effect of the Jovian oblateness on Pioneer 10/11 Radio occultations. *Geophys. Res. Lett. 2*, 265–266.

Hunten, D. (ed.). (1974). *The Atmosphere of Titan. NASA SP-340*, NASA, Washington D.C. 185 pp.

Kliore, A., Cain, D., Levy, G., Eshleman, V., Drake, F., and Fjeldbo, G. (1965). The Mariner 4 occultation experiment. *Astronaut. Aeronaut 3*, 72–80.

Kliore, A., and Woiceshyn, P. (1976). Structure of the atmosphere of Jupiter from Pioneer 10 and 11 radio occultation measurements. In *Jupiter* (T. Gehrels, ed.), pp 216–237. University of Arizona Press, Tucson.

Marouf, E. (1975). The rings of Saturn: Analysis of a bistatic-radar experiment. Ph.D. dissertation. *Technical Report 3240-1 SU SEL 75-006*, Stanford Electronics Laboratories, Stanford University, Stanford, CA.

Pollack, J., Summers, A., and Baldwin, B. (1973). Estimates of the size of the particles in the rings of Saturn and their cosmogonic implications. *Icarus 20*, 263–278.